Journal of Statistical Physics, Vol. 44, Nos. 5/6, 1986

Study of a High-Dimensional Chaotic Attractor

Kensuke Ikeda[1] **and Kenji Matsumoto**[2]

Received December 26, 1986

The nature of a very high-dimensional chaotic attractor in an infinite-dimensional phase space is examined for the purpose of studying the relationships between the physical processes occurring in the real space and the characteristics of high-dimensional attractor in the phase space. We introduce two complementary bases from which the attractor is observed, one the Lyapunov basis composed of the Lyapunov vectors and the another the Fourier basis composed of the Fourier modes. We introduce the "exterior" subspaces on the basis of the Lyapunov vectors and observe the chaotic motion projected onto these exteriors. It is shown that a certain statistical property of the projected motion changes markedly as the exterior subspace "goes out" of the attractor. The origin of such a phenomenon is attributed to more fundamental features of our attractor, which become manifest when the attractor is observed from the Lyapunov basis. A counterpart of the phenomenon can be observed also on the Fourier basis because there is a statistical one-to-one correspondence between the Lyapunov vectors and the Fourier modes. In particular, a statistical property of the high-pass filtered time series reflects clearly the difference between the interior and the exterior of the attractor.

KEY WORDS: Chaos; turbulence; high-dimensional chaotic attractor; attractor interior; attractor exterior; Lyapunov basis; Fourier basis; Lyapunov component; Lyapunov spectrum; Fourier component; high-pass filter; intermittency.

1. INTRODUCTION

Study of chaos in dissipative open systems has developed considerably over the past 10 years. In particular, chaos in systems with a few degrees of freedom has been examined extensively from various points of view.[1] On the contrary, however, study of chaotic behavior in systems with infinite

[1] Research Institute for Fundamental Physics, Kyoto University, Kyoto 606, Japan.
[2] Faculty of Pharmaceutical Sciences, Hokkaido University, Sapporo 060, Japan.

0022-4715/86/0900-0955$05.00/0

degrees of freedom has not progressed substantially. The chaotic behavior immediately after its birth can be described by a small number of degrees of freedom even when the system itself has infinite degrees of freedom.[2] However, the chaotic state realized by a sufficiently large amount of energy injection from the external world has, in general, contributions from an extremely large number of degrees of freedom. A classical example is the fully developed fluid turbulence. Traditional studies of fluid turbulence have developed statistical theories which provide methods to compute statistical quantities such as correlation function, Fourier spectrum, and so on.[3] These theories, however, have been constructed without inquiring of the mechanical origin of randomness in turbulent behavior. To elucidate this problem it is necessary to study the dynamical structure of the attractor into which the orbit in the phase space is trapped, but the dimension of the subspace confining the attractor is too large to find an efficient method to recognize such a high-dimensional object in the phase space. This is the reason why there has not been a clear understanding of the connection between turbulent behavior occurring in real physical space with the structure of the attractor in phase space.

Is it possible to recognize the dynamical structure of a high-dimensional attractor? Are there fundamental relations between the physical processes in real space and the structure of attractor in phase space? Several authors have attempted to study high-dimensional chaotic state exhibited by simple dynamical systems with infinite degrees of freedom.[4,5] They succeeded in computing various quantities such as Lyapunov spectrum, Lyapunov dimension, metric enropy, and so on, which characterize some aspects of attractors. Unfortunately, however, we are not aware of any previous approach that provides insight into the nature of high-dimensional attractors which may even partly answer the above questions.

Let us consider an open dissipative system with infinite degrees of freedom. Even in the chaotic state, most of the degrees of freedom do not actively contribute to sustaining chaotic behavior; rather they work as a "sink" for fluctuation. We roughly call the subspace spanned by the modes actively contributing to the chaotic behavior the "interior" of attractor. On the contrary, the subspace spanned by the inactive "sink" modes may be called the "exterior" of attractor. The chaotic orbit in the phase space is unstable against an infinitesimal fluctuation, and a small error is amplified exponentially along it. This fact means the chaotic orbit has an ability to produce new information. It is in the interior that the new information can be generated. The information produced in the interior is transported to the exterior of the attractor and dies away there. Therefore, it is expected that the dynamical behavior in the exterior should be qualitatively different from that in the interior. If we can embed the attractor into a space of finite

dimension by a smooth transformation, this subspace is just the interior. However, such an operation is at least practically impossible considering that the attractor is "strange" in the sense that it is composed of an infinite number of "sheets." It may be possible, however, to construct a subspace that can approximately confine the attractor.

The subject of the present paper is concerned with the problem described above. Our first question is whether there is some method to decompose the phase space into the two subspaces; the interior and the exterior of attractor. The second question is how the dynamical behavior is different qualitatively in the interior and in the exterior. The final question is in what physical process we can recognize the qualitative difference. We investigate these questions by analyzing a very high-dimensional chaotic attractor exhibited by a mathematically simple and physically realistic dynamical model with infinite degrees of freedom.

The outline of our paper is as follows. In Section 2 we introduce a simple model equation, which we investigate in detail. The physical and mathematical meanings of the model equation are briefly reviewed. The instability process through which the linear fluctuation modes are successively excited is explained. In Section 3 we introduce two kinds of fundamental bases from which we watch the chaotic motion trapped in the attractor, one the Lyapunov basis composed of Lyapunov vectors, the other the Fourier basis based on the Fourier modes. In Section 4 we show an important relation between the Lyapunov spectrum of chaotic state and the decay rate spectrum of linear fluctuation modes. In Section 5 we watch the attractor from the Lyapunov basis and point out that the global shape of attractor is closely related with the Lyapunov spectrum. We introduce in Section 6 the idea of the "exteriors" of attractor as subspaces spanned by the Lyapunov vectors. We study the statistical properties of the chaotic motion projected onto the exteriors. A certain statistical property exhibits a notable change as the exterior subspace goes out of the attractor. The origin of such a behavior is explained using the results of both Sections 4 and 5. In Section 7 it is shown that each base vector of the Lyapunov basis has a one-to-one correspondence with each of the Fourier vectors in a statistical sense. Thus it is anticipated that the counterpart of the phenomena discussed in Section 6 can be observed also in the Fourier basis. This is verified in Section 8, where it is shown that the high-pass filtered time series enables us to recognize the qualitative difference between the dynamics of the interior and those of the exterior. In Sections 4–8 the main results of each section are briefly summarized at the end of each section. Finally, Section 9 is devoted to the summary and conclusion of the present paper.

We by no means intend to assert that the results presented here are

universal. However, we believe that the approach used in the present paper can usefully be applied to understanding any high-dimensional attractor in a system with infinite degrees of freedom.

2. MODEL SYSTEM

To accomplish our purpose it is desired that the model system should have a simple mathematical structure and, furthermore, should have a clear physical meaning. For this reason we use a delay-differential (DD) equation, i.e., a differential equation involving a time-delayed feedback

$$dx(t)/dt = -x(t) + \pi\mu f[x(t - t_R)] \tag{2.1}$$

In the present paper we use the following form of the feedback function

$$f(x) = \sin(x - x_0) \tag{2.2}$$

The model equation (2.1) together with (2.2) have been proposed as a standard model of "optical turbulence" in nonlinear optical resonators.[6] They have been derived from a set of nonlinear partial differential equations (Maxwell–Bloch equations) for space and time under some appropriate conditions. A great advantage of eq. (2.1) is that it can be regarded as a mapping rule from a "spatial pattern" to a new pattern after a finite time interval t_R, as will be explained later. Thus the CPU time required for integrating eq. (2.1) numerically is much shorter (about 10^{-3} times) than that required for usual partial differential equations. The model equation (2.1) has two principal bifurcation parameters, t_R and μ. Physically, the delay time t_R comes from the boundary condition imposed upon the optical resonator and is related to the system size (i.e., the length of optical resonator), whereas μ means the energy injected in the system and plays a similar role as the Reynolds number in fluid turbulence. The effect of parameter x_0 is trivial. Thus we fix this $x_0 = 0$ from now on.

For sufficiently large μ (and/or t_R) the stationary solution x_s of eq. (2.1) becomes unstable as μ (and/or t_R) increases, and finally leads to a chaotic solution. It will be instructive to study the process of instability in some detail.[6] Linearizing eq. (2.1) around x_s and setting $x(t) - x_s \propto e^{i\Omega t}$, we immediately obtain a characteristic equation for the complex frequency $\Omega = \pm\beta - i\alpha$ ($\beta > 0$) of a linear fluctuation mode

$$i\Omega + 1 = \pi\mu f'(x_s) \exp(-i\Omega t_R) \tag{2.3}$$

Since eq. (2.1) is a system with infinite degrees of freedom, eq. (2.3) has infinite number of roots corresponding to the frequencies of linear fluc-

tuation modes. We number the modes in order of the magnitude of β. It is easy to show that β_n, i.e., the β of nth mode, satisfies

$$2n\pi/t_R < \beta_n < (2n+1)\pi/t_R \tag{2.4}$$

The frequency of the modes are distributed with almost equal intervals $\approx 2\pi/t_R$. In terms of laser physics these modes are the longitudinal cavity modes in resonance with the optical resonator surrounded by two mirrors with spacing $t_R c$ (c light velocity; see Section 3). For sufficiently large n, the linear fluctuation mode becomes stable, and its frequency and decay rates are asymptotically expressed by

$$\beta_n \to (2n+\tfrac{1}{2})\pi/t_R \tag{2.5a}$$

$$\alpha_n \to -\log[\beta_n/|\pi\mu f'(x_s)|]/t_R \tag{2.5b}$$

However, not all the linear modes are stable if $|\pi\mu f'(x_s)| > 2$. The nth mode becomes unstable each time μ (or t_R) exceeds the critical value $\mu^{(n)}$ (or $t_R^{(n)}$). Since $\mu^{(n+1)} > \mu^{(n)}$ ($t_R^{(n+1)} > t_R^{(n)}$) the number of unstable modes increases with μ (and/or t_R) as shown schematically in Fig. 1. Thus the number of

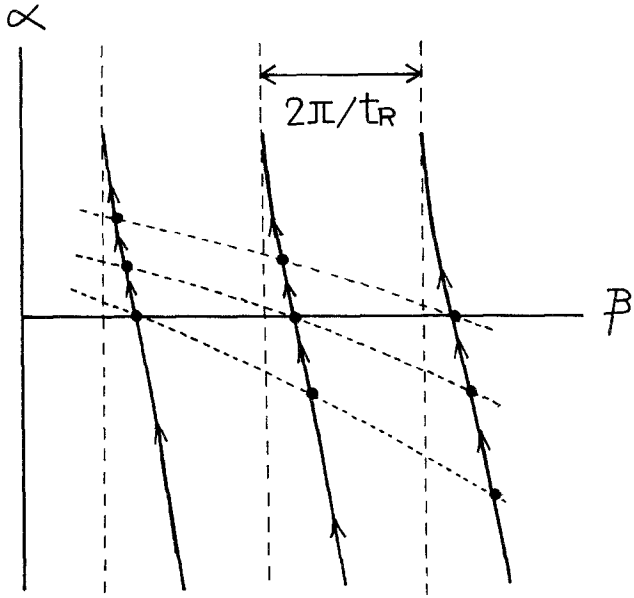

Fig. 1. Motion of complex characteristic frequency $\Omega_n = \beta_n - i\alpha_n$. The broken curves connect (α_n, β_n) of the same values of t_R and μ. (α_n, β_n) moves in the direction indicated by an arrow as t_R and/or μ is increased.

unstable modes responsible for the self-oscillation increases with μ (and/or t_R). If the self-oscillation is chaotic, the above fact implies that the dimension of chaos can be made arbitrarily large by controlling μ and/or t_R.

Let us divide the time domain into sections of interval t_R, i.e., $I_n = (nt_R, (n+1)t_R]$ $(n=0, 1, 2,...)$. Next we denote the solution $x(t)$ in the section I_n by $x_n(t)$, where $\tau \equiv t - nt_R$ $(0 \leqslant \tau < t_R)$. Then eq. (2.1) is rewritten as

$$x_{n+1}(\tau) = e^{-\tau} x_n(t_R) + \pi\mu \int_0^\tau e^{-\tau+s} f[x_n(s)]\, ds \tag{2.6}$$

Now we consider an infinite-dimensional "state vector" $\mathbf{R}_n$ whose component at τ $(0 \leqslant \tau < t_R)$ is given by $x_n(\tau)$. Then eq. (2.6) defines an *infinite-dimensional mapping rule* from $\mathbf{R}_n$ to $\mathbf{R}_{n+1}$.

$$\mathbf{R}_{n+1} = F(\mathbf{R}_n) \tag{2.6}'$$

Next we consider how the infinitesimal variation $\delta x_n(\tau)$ around the solution $x_n(\tau)$ develops. Linearizing eq. (2.6) around $x_n(\tau)$, we have

$$\delta x_{n+1}(\tau) = e^{-\tau} \delta x_n(t_R) + \pi\mu \int_0^\tau ds\, e^{-\tau+s} f'[x_n(s)]\, \delta x_n(s) \tag{2.7}$$

which defines a mapping rule for the infinitesimal vector $\delta\mathbf{R}_n \equiv \{\delta x_n(\tau)\}$ in the tangent space

$$\delta\mathbf{R}_{n+1} = DF(\mathbf{R}_n)\, \delta\mathbf{R}_n \tag{2.7}'$$

The numerical methods used for integrating eq. (2.6) and eq. (2.7) are explained in Appendix A.

3. TWO FUNDAMENTAL BASES

In this section we introduce two kinds of fundamental bases from which we observe the motion of system trapped in the attractor. One is called the Lyapunov basis and another the Fourier basis, as explained below.

3.1. Lyapunov Basis

Let us consider a unit sphere $|\delta\mathbf{R}_0| = 1$ in the tangent space of a state vector $\mathbf{R}_0$ in the attractor $\hat{A}$. The Nth iteration of the sphere evolves into an ellipsoid, because the Nth iteration $\delta\mathbf{R}_N = DF(\mathbf{R}_N) \cdot DF(\mathbf{R}_{N-1}) \cdot \cdots DF(\mathbf{R}_1) \cdot \delta\mathbf{R}_0 \equiv D^N F.\ \delta\mathbf{R}_0$ satisfies $\delta\mathbf{R}_N^t (D^N F^{-1})^t (D^N F^{-1})\, \delta\mathbf{R}_N = 1$. Con-

sider the limit $N \to \infty$. Then the length of any principal axis of the ellipsoid asymptotically grows (or decays) like $\exp(N\lambda)$. The characteristic exponent λ is usually called the Lyapunov exponent.[7,8] Hereafter, we number the Lyapunov exponents in order of their magnitudes, i.e., $\lambda_1 \geqslant \lambda_2 \geqslant \lambda_3 \geqslant \cdots \geqslant \lambda_i \geqslant \cdots$. The set of Lyapunov exponents $(\lambda_1, \lambda_2, ..., \lambda_n, ...)$ is called the Lyapunov spectrum. On the other hand, a unit vector taken along the principal axis corresponding to λ_i is called the ith Lyapunov vector $\mathbf{e}_i(\mathbf{R}_N)$. We call the set of Lyapunov vectors $\{\mathbf{e}_i(\mathbf{R})\}$ the Lyapunov basis at $\mathbf{R}$.

Next, we define the Lyapunov component as an inner product of the state vector $\mathbf{R}$ with the Lyapunov basis $\mathbf{e}_i(\mathbf{R}')$ at $\mathbf{R}' \in \hat{A}$

$$C_i(\mathbf{R} \mid \mathbf{R}') = \mathbf{R} \cdot \mathbf{e}_i(\mathbf{R}') = \int_0^{t_R} d\tau\, y(\tau)\, e_i(\tau \mid \mathbf{R}') \tag{3.1}$$

where $y(\tau)$ and $\mathbf{e}_i(\tau \mid \mathbf{R}')$ are the components of the state vector $\mathbf{R}$ and of the Lyapunov vector $\mathbf{e}_i(\mathbf{R}')$ at the time $(0 < \tau \leqslant t_R)$, respectively.

The Lyapunov vectors together with the Lyapunov exponents represent the local structure of the attractor; in the directions of $\mathbf{e}_i(\mathbf{R}')$ the attractor is expanded (or shrunk) with a rate related to the factor e^{λ_i}. In this sense the Lyapunov basis is looked upon as a *dynamical coordinate system*. A defect of the Lyapunov basis is that it is not unique but depends on the state vector $\mathbf{R}'$ at which the Lyapunov basis is defined. To avoid this complication we later redefine various quantities defined in connection with the Lyapunov basis at $\mathbf{R}'$ as the averaged ones over $\mathbf{R}' \in \hat{A}$.

A conventional method for computing the Lyapunov vectors together with the Lyapunov exponents is the Gram–Schmidt orthogonalization procedure. In Appendix A we review briefly how this procedure can be applied to the DD equation.[4,8]

3.2. Fourier Basis

The Fourier basis $\{\mathbf{f}_k\}$ $(k = 0, 1, 2, ...)$ is a set of vectors whose component $f_k(\tau)$ at time $(0 < \tau \leqslant t_R)$ is given by

$$\begin{aligned} f_k(\tau) &= (2/t_R)^{1/2} \cos \omega_k \tau \qquad (k = \text{even}) \\ &= (2/t_R)^{1/2} \sin \omega_{k+1} \tau \qquad (k = \text{odd}) \end{aligned} \tag{3.2}$$

where $\omega_k \equiv k\pi/t_R$ is defined so as to fulfill the periodic boundary condition. The inner product of the state vector $\mathbf{R}$ with a Fourier basis $\mathbf{f}_k$, i.e.

$$F_k(\mathbf{R}) \equiv \mathbf{R} \cdot \mathbf{f}_k = \int_0^{t_R} d\tau\, y(\tau)\, f_k(\tau) \tag{3.3}$$

is called the Fourier component.

The Fourier vector $\mathbf{f}_k$ has a strong resemblance to the linear fluctuation mode with frequency β_k (eq. (2.4)). Thus the Fourier component measures the contribution of the linear fluctuation mode to the chaotic motion. Our system physically describes the variation of the phase of electric field at a fixed position in a nonlinear optical resonator. In such an optical system the spatial pattern moving with the light velocity is observed as a temporal pattern at a fixed position. Therefore, the Fourier decomposition in the time domain is equivalent to that in the space domain; in other words, the vectors $\mathbf{f}_k$ may be interpreted as the spatial Fourier modes. Specifically, in systems described by partial differential equations in space and time it will be quite natural to define the Fourier vector by the spatial Fourier modes. Thus the physical meaning of the Fourier basis is very clear, and this basis can be thought of as a *physical coordinate system* in contrast to the Lyapunov basis.

Unfortunately the time series $y(\tau)$ does not satisfy the periodic boundary condition and the high-frequency Fourier component involves a spurious algebraic decay accompanied by Gibbs oscillation. To suppress this undesired effect the time series is always multiplied by a cosine-bell window

$$\begin{aligned} B(\tau) &= [1-\cos(\pi\tau/\Delta)]/2 && (\tau \leqslant \Delta) \\ &= 1 && (\Delta \leqslant \tau \leqslant t_R - \Delta) \\ &= \left[1-\cos\left\{\frac{\pi(\tau - t_R)}{\Delta}\right\}\right]\Big/2 && (\tau \leqslant t_R - \Delta) \end{aligned}$$

in computing the Fourier component. If the width Δ is taken large enough, say $\Delta \gg t_R/32$, the results are insensitive to the choice of Δ.

4. LYAPUNOV SPECTRUM

By the Gram–Schmidt procedure in Appendix A we can compute the Lyapunov exponents as well as the Lyapunov vectors. Once the Lyapunov spectrum is obtained, we can evaluate the Lyapunov dimension introduced by Kaplan and Yorke[9]

$$D = \bar{D} + \sum_{i=1}^{\bar{D}} \lambda_i / |\lambda_{\bar{D}+1}| \tag{4.1}$$

where $\bar{D}$ is the largest integer for which $\sum_{i=1}^{\bar{D}} \lambda_i > 0$. This quantity is the dimension of the volume element in the tangent space that makes the volume expansion rate $\exp \sum_{i=1}^{j} \lambda_i$ invariant and so it provides a measure of the dimension of attractor. Recently, Farmer computed the Lyapunov spectrum of a DD equation of the same class as eq. (2.1).[4] He also com-

puted the fractal dimension D_F directly by the box-counting method when D_F is not very large and compared D_F with D obtained by eq. (4.1), finding that D is very close to D_F. Thus it is conjectured that D can be used as an approximate value of D_F. Hereafter we use D as the measure of the dimension of attractor.

An example of Lyapunov spectrum is depicted in Fig. 2(a), where D is estimated to be about 45 in this case. Empirical studies for the model equation (2.1) reveals that there are simple scaling rules for the Lyapunov spectrum. For $t_R \gg 1$ and μ large enough ($\mu \gtrsim 0.85$) we have a scaling rule $\lambda_i(t_R, \mu) = \lambda_{i/t}(1, \mu)$ with respect to the system size t_R so that D is proportional to t_R. The latter property has already been obtained by Farmer.[4] Existence of a similar scaling rule has been found also for a partial differential equation.[5] Thus, the scaling rule of Lyapunov spectrum with respect to the system size appears to be quite universal. In the case of our system, a further scaling rule with respect to μ exists, i.e., $\lambda_i(t_R, \mu) = \lambda_{i/\mu}(t_R, 1)$ for $\mu \gg 1$ and $i \gg t_R/\pi$. Thus D is proportional to μ, too, for $\mu \gg 1$. The asymptotic expression is empirically given by

$$D \approx (1.10 \pm 0.05)\, t_R \mu \tag{4.2}$$

At first sight, increases in μ and t_R bring about similar effect on making the chaotic behavior more complicated. The role of μ and t_R is, however, quite different; Let us consider the metric entropy H of the chaotic state. The metric entropy, which measures the uncertainty (or information) produced per unit time, is roughly the total sum of the positive Lyapunov exponents.

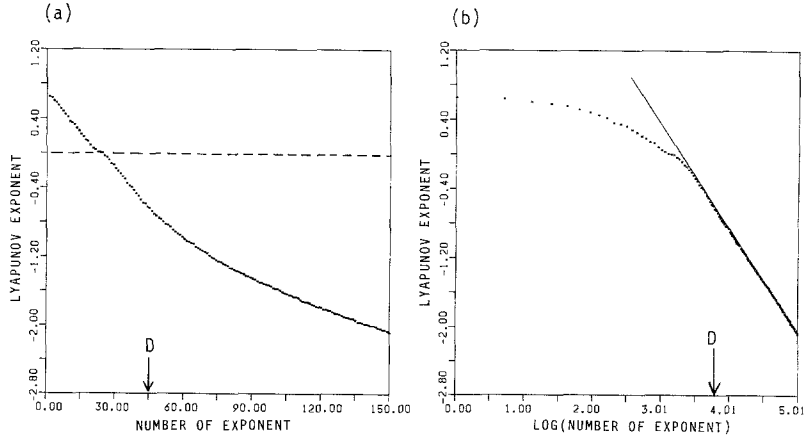

Fig. 2. An example of Lyapunov spectrum. In (b) the line indicates the asymptotic log-linear behavior. Here $\mu = 2.10$ and $t_R = 20$.

Since our Lyapunov exponent is defined at every t_R, H should be redefined as Σ (positive Lyapunov exponent)$/t_R$. Obviously H depends only on μ and is independent of t_R because of the scaling relations. In particular $H \propto \mu$ for $\mu \gg 1$. Thus the complexity of the chaotic state, which is invariant for the change of t_R, is enhanced only by increasing μ. In our system it can be proven that in the limit of $\mu \gg 1$ the time series becomes so complicated as to be described by a Gaussian stochastic process.[7][3] This fact seems to be consistent with the above considerations. An advantage of our system is that a variety of chaotic states with the same D but with different complexities can be produced by adjusting the two parameters μ and t_R appropriately.

The linear fluctuation modes introduced in Section 2 play active roles in generating chaotic behaviors if they are in or near the unstable band. However, stable modes far from the unstable band are not excited substantially because their decay rate α_i gets larger like $\log i$. These modes should be responsible for the large negative Lyapunov exponents. The temporal behavior of the stable modes is dominated by the self-decaying motion with the decay rate α_i, so that the Lyapunov exponent corresponding to these mode should agree with α_i. Indeed, as shown in Fig. 2(b), the Lyapunov spectrum approaches a log linear behavior as the number of Lyapunov exponent i increases

$$\lambda_i \to -\log i + \text{const.} \tag{4.3}$$

which agrees with the decay rate spectrum of the linear fluctuation modes eq. (2.5b). This log dependence is observed also by Farmer.[4]

A quite interesting fact is that there exists a clear "critical number" $i = I_{LE}$ above which λ_i exhibits the log linear behavior. I_{LE} should characterize the upper bound of the mode number for which nonlinearity plays an essential role. Thus we may expect that I_{LE} may have something to do with the Lyapunov dimension. Indeed, as is shown in Fig. 3, there is a clear linear relation between I_{LE} and D

$$I_{LE} = 0.65\, D \tag{4.4}$$

This relation holds quite well for any set of parameters t_R and μ. Thus we can summarize the most important result in this section as follows

[3] (In our system the largest Lyapunov exponent is related to the correlation function of the delayed force as

$$\lambda_1 = \log \left[(\pi\mu)^2 \int_0^\infty \langle\langle f[x(s)]\, f[x(0)] \rangle\rangle\, ds \right] \Big/ 2 \approx (\log 1.57\mu)/2$$

K. Ikeda, unpublished.)

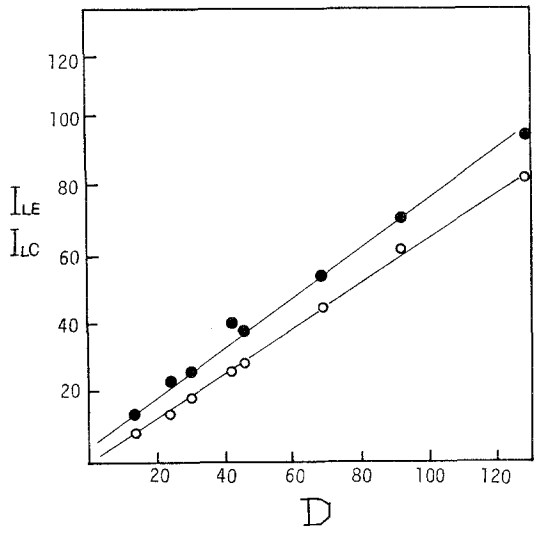

Fig. 3. Relations of the characteristic numbers I_{LE}(○) and I_{LC}(●) to the Lyapunov dimension D for various sets of values of (t_R, μ).

Short Summary 1. There is a critical number I_{LE} *above which the Lyapunov spectrum agrees with the decay rate spectrum of the linear fluctuation modes.* I_{LE} *is closely connected with the dimension of the strange attractor.*

We have to note that there is no reason why I_{LE} should be close to D. Recently, the Lyapunov spectrum of the Kuramoto–Sivashinski (KS) equation has been studied by Pomeau, Pumir, and Pelce.[5] Judging from their numerical data, I_{LE} seems to be considerably larger than D, but if I_{LE} exists, we conjecture that it is proportional to D also in their case.

5. LYAPUNOV COMPONENT

How does the attractor look when it is observed from the Lyapunov basis? Let us consider a square root average of the Lyapunov component over the state vector, i.e.

$$C_i(\mathbf{R}') = [\langle\langle C_i^2(\mathbf{R} \mid \mathbf{R}')\rangle\rangle_{\mathbf{R} \in \hat{A}}]^{1/2} \tag{5.1}$$

where the notation $\langle\langle \cdots \rangle\rangle_{\mathbf{R} \in \hat{A}}$ indicates an average over the state vector $\mathbf{R}$ moving in the attractor $\hat{A}$. This quantity represents the size of attractor measured along the ith Lyapunov vector and thus characterizes the global shape of the attractor observed from a local Lyapunov basis. This quantity,

however, still depends on the position $\mathbf{R}'$ at which the Lyapunov basis is defined. Hence we further average $C_i^2(\mathbf{R}')$ with respect to $\mathbf{R}' \in \hat{A}$

$$C_i = [\langle\langle C_i^2(\mathbf{R} \mid \mathbf{R}')\rangle\rangle_{\mathbf{R},\mathbf{R}' \in \hat{A}}]^{1/2} \tag{5.2}$$

We call this quantity the averaged Lyapunov component.

As mentioned in Section 3, the Lyapunov exponents characterize the local structure of attractor. In particular the local width of attractor measured in the direction of the ith Lyapunov vector is related to the factor e^{λ_i}. Thus C_i, which represents the size of the attractor, might have some connection with the local width. Indeed the result of numerical simulation suggests that the Lyapunov component exhibits quite similar behavior as the factor e^{λ_i} as expressed in the simple relation

$$C_i \propto e^{\lambda_i \eta} \tag{5.3}$$

An example is depicted in Fig. 4. For $i > D$ the exponent η is constant independent of i with magnitude between 1 and 2, and seems to approach 1 as $\mu \to \infty$. For $i < D$ the exponent becomes slightly dependent upon i, but this dependence is much less significant than the dependence of e^{λ_i} on i. Therefore, there is a characteristic number corresponding to I_{LE} above which C_i exhibits a log-linear behavior

$$\log C_i = -\eta \log i + \text{const.} \tag{5.4a}$$

or

$$C_i \propto i^{-\eta} \tag{5.4b}$$

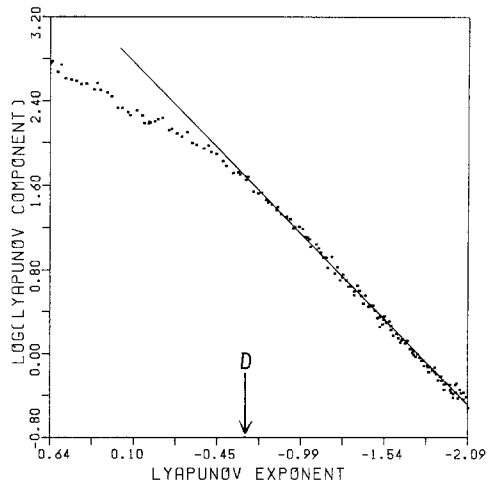

Fig. 4. Relation between the Lyapunov exponents and the Lyapunov components. The line is a guide for eyes. Here $\mu = 2.10$ and $t_R = 20$.

The characteristic vector number I_{LC} is slightly different from I_{LE} because the exponent η depends weakly on i for $i < D$. As shown in Fig. 3 the plots of I_{LC} and D are well-fitted with a linear function

$$I_{LC} = 0.70D + 6.0 \tag{5.5}$$

for any set of parameters μ and t_R. Thus I_{LC} is slightly larger than I_{LE}. We note that eq. (5.4b) provides the lower bound for η, i.e., $\eta > 1$ because $\langle\langle \mathbf{R} \cdot \mathbf{R} \rangle\rangle = \sum C_i^2 < +\infty$. Now we summarize the result of this section:

Short Summary 2. In log scale the averaged Lyapunov components are quite similar to the Lyapunov spectrum. Hence, there is a characteristic vector number I_{LC} *corresponding to* I_{LE} *above which the Lyapunov components in log scale behaves like the decay rates of the linear fluctuation modes.*

6. EXTERIORS OF ATTRACTOR AND PROJECTION ONTO IT

Consider a set of Lyapunov vectors $\{\mathbf{e}_i(\mathbf{R}')\}$ defined at a position $\mathbf{R}'$ in the strange attractor. We define a subspace $IN_l^L(\mathbf{R}')$ which is spanned by all the Lyapunov vectors whose vector number is smaller than l, i.e., $\mathbf{e}_1(\mathbf{R}')$, $\mathbf{e}_2(\mathbf{R}')$,..., $\mathbf{e}_{l-1}(\mathbf{R}')$. This subspace "confines" the attractor in the vicinity of $\mathbf{R}'$ if the vector number l is chosen to be larger than D. Conversely, the complementary subspace $EX_l^L(\mathbf{R}')$ spanned by the vectors $\mathbf{e}_l(\mathbf{R}')$, $\mathbf{e}_{l+1}(\mathbf{R}')$, $\mathbf{e}_{l+2}(\mathbf{R}')$,... "excludes" the attractor in the vicinity of $\mathbf{R}'$. This subspace, of course, does not exactly exclude the whole of the attractor because the subspace $IN_l^L(\mathbf{R}'')$ confining the attractor locally at $\mathbf{R}''$ rotates in the phase space as $\mathbf{R}''$ goes away from $\mathbf{R}'$ and it becomes not perpendicular to $EX_l^L(\mathbf{R}')$. It seems, however, that the subspace which is effectively covered by $IN_l^L(\mathbf{R}'')$ as $\mathbf{R}''$ moves in the attractor does not substantially occupy the whole of phase space, i.e., it has small finite dimension. To verify this we have done the following computation.

Taking the two Lyapunov vectors $\mathbf{e}_i(\mathbf{R}')$ and $\mathbf{e}_j(\mathbf{R}'')$ defined at different state vectors $\mathbf{R}'$ and $\mathbf{R}''$ in $\hat{A}$, we computed the square average of the inner product

$$Q_L(i|j) = \langle\langle (\mathbf{e}_i(\mathbf{R}') \cdot \mathbf{e}_j(\mathbf{R}''))^2 \rangle\rangle_{\mathbf{R}', \mathbf{R}'' \in \hat{A}}$$

moving $\mathbf{R}'$ and $\mathbf{R}''$ independently in $\hat{A}$. An example is depicted in Fig. 5. In this figure a circle indicates the value of $j = j_{\max}(i)$ maximizing $Q_L(i|j)$ for a given i. For very small i, $j_{\max}(i)$ is equal to 1. Such vectors are called the "core Lyapunov vectors," which will be discussed in the next section and in Appendix B. Except for the core vectors, $j_{\max}(i)$ is located in the vicinity of i. This fact implies that the order of the Lyapunov vectors $\{\mathbf{e}_i(\mathbf{R}')\}$ is

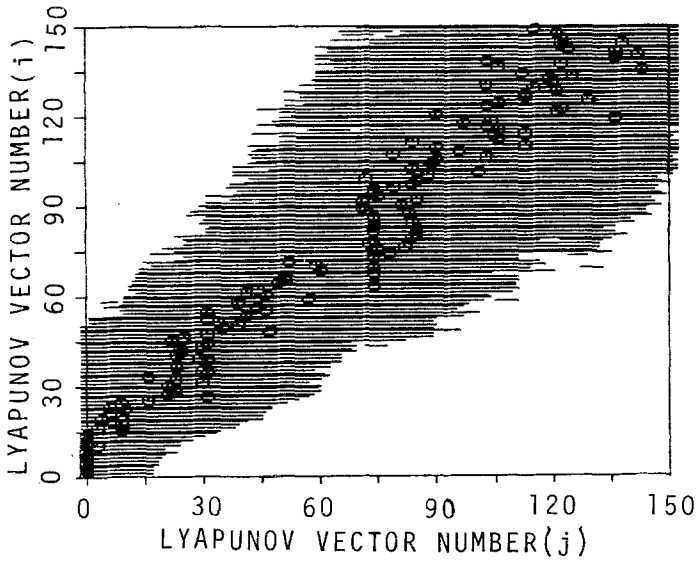

Fig. 5. Relation between two Lyapunov vectors $\mathbf{e}_i(\mathbf{R}')$ and $\mathbf{e}_j(\mathbf{R}'')$ defined at different state vectors $\mathbf{R}'$ and $\mathbf{R}''$ in the attractor. Here $\mu = 2.89$ and $t_R = 20$. (See text.)

almost preserved in a statistical sense as the state vector $\mathbf{R}'$ moves in $\hat{A}$. Next we consider the fluctuation of a Lyapunov vector of a given vector number. In Fig. 5 the shaded region indicates the set of j satisfying $Q_L(i|j) \geqslant 0.5 \times Q_L[i|j_{\max}(i)]$ for each i. This region represents the number j of the Lyapunov vectors $\mathbf{e}_j(\mathbf{R}'')$ effectively spanning the subspace over which the vector $\mathbf{e}_i(\mathbf{R}')$ wanders as $\mathbf{R}'$ moves in A away from $\mathbf{R}''$. Evidently such js are localized around $j_{\max}(i) = i$. Thus the Lyapunov vectors defined at different state vectors in $\hat{A}$ are considerably correlated if their vector numbers are close to each other.

We do not assert that the above results are generic for all attractors. However, we conjecture that they are valid for the Lyapunov vectors with sufficiently large vector numbers. The problem is the total number of core vectors. In our attractor the total number of core vectors is fortunately (or maybe unfortunately) much smaller than D, so that most of the Lyapunov vectors $\mathbf{e}_l(\mathbf{R}')$ with $l \lesssim D$ are "well-ordered" over the attractor. This is not the case for all attractor. We conjecture that a counterexample is the Kuramoto–Sivashinsky equation. Judging from the results of Pomeau, Pumir, and Pelce[5] the total number of core vectors seems to be larger than D.

In addition to being well-ordered, the motion of a Lyapunov vector of a given number is effectively restricted to a subspace of small dimension.

Thus we can make the subspace $IN_l^L(\mathbf{R}')$ so as to *effectively* confine the whole of the attractor by choosing l sufficiently large. Therefore, the complementary subspace $EX_l^L(\mathbf{R}')$ may be looked upon as an *exterior* subspace excluding the attractor.

We consider the projection of a state vector $\mathbf{R}$ onto the lth exterior $EX_l^L(\mathbf{R}')$

$$\hat{P}_l^L(\mathbf{R}')\mathbf{R} = \sum_{j \geqslant l} C_j(\mathbf{R} \mid \mathbf{R}')\, \mathbf{e}_j(\mathbf{R}') \tag{6.1}$$

where $\hat{P}_l^L(\mathbf{R}')$ is the projection operator. If l is much smaller than D, the exterior $EX_l^L(\mathbf{R}')$ contains a considerable part of the attractor, so that the projected vector $\hat{P}_l^L(\mathbf{R}')\mathbf{R}$ contains rich information from the inside of the attractor. For $l \gg D$, however, $EX_l^L(\mathbf{R}')$ goes out of the attractor and the projected vector contains only the information from the outside of the attractor. We are interested in how the characteristics of the projected vector vary when the order l is increased across dimension D.

The component of the projected vector at time τ, which is denoted by $\psi_l(\tau, \mathbf{R} \mid \mathbf{R}')$, is

$$\psi_l(\tau, \mathbf{R} \mid \mathbf{R}') = \sum_{j \geqslant l} C_j(\mathbf{R} \mid \mathbf{R}')\, e_j(\tau \mid R') \tag{6.2}$$

where $e_j(\tau \mid \mathbf{R}')$ is the component of $\mathbf{e}_j(\mathbf{R}')$ at τ. Now we show that the statistical properties of the amplitudes of ψ_l change markedly as l exceeds some characteristic number. For this purpose we introduce a correlation function between the amplitudes of two time series ψ_l^2 and ψ_m^2, each of which is normalized by its time average

$$C_{lm}^L \equiv \ll [\psi_l^2(\tau, \mathbf{R} \mid \mathbf{R}')/\overline{\psi_l^2(\tau, \mathbf{R} \mid \mathbf{R}')}][\psi_m^2(\tau, \mathbf{R} \mid \mathbf{R}')/\overline{\psi_m^2(\tau, \mathbf{R} \mid \mathbf{R}')}] \gg_{\mathbf{R}, \mathbf{R}' \in \hat{A}} - 1 \tag{6.3}$$

where the bar indicates a time average

$$\bar{F} \equiv t_R^{-1} \int_0^{t_R} F(t')\, dt'$$

In Fig. 6(a) the correlation functions for various l are depicted as a function of m. The correlation function has the maximum at $m = l$ and decreases monotonically as $|m - l|$ increases, so that we can define the half-width $\Delta_L(l)$ of the correlation function as the difference of two values of m satisfying $C_{lm}^L = C_{ll}^L/2$. $\Delta_L(l)$ measures the total number of ψ_m^2 correlated with ψ_l^2. Fig. 6(b) shows the typical behavior of $\Delta_L(l)$. A remarkable characteristic is that $\Delta_L(l)$ increases suddenly as l exceeds a threshold value. This threshold agrees well with I_{LC} introduced in the previous section.

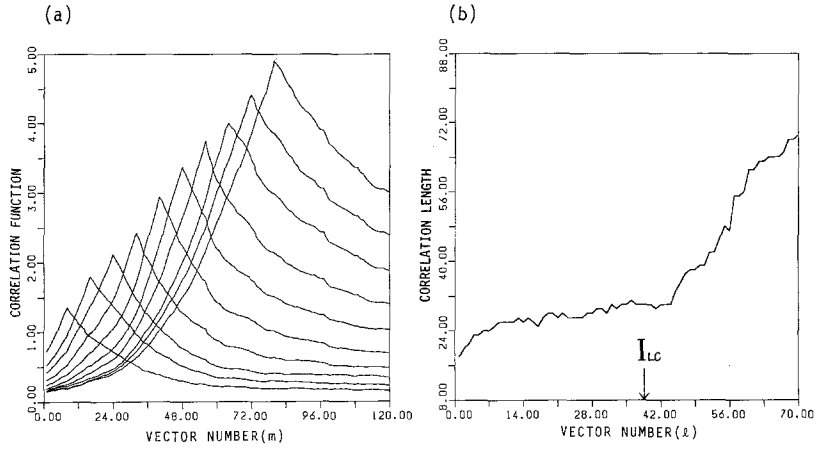

Fig. 6. (a) Correlation functions C_{lm}^L at various l, and (b) correlation length $\Delta_L(l)$. In (a) each C_{lm}^L takes the maximum value at $m=l$ and the peak value C_{ll}^L indicates (flatness factor -1) at l. Here $\mu=2.10$ and $t_R=20$.

What are the origins of such behavior? We point out at least two origins. One is the transition to the log linear behavior seen in the Lyapunov component, but another is a quite new effect; it is a localization effect of the projected vector in the time domain. We first explain the former effect.

Let θ_{lm} be the angle between two projected vectors $\hat{P}_l^L(\mathbf{R}')\mathbf{R}$ and $P_m^L(\mathbf{R}')\mathbf{R}$. The square average of $\cos\theta_{lm}$, i.e., the inner product of the two projected vectors, measures the similarity between two projected vectors. It is expressed only in terms of the Lyapunov components

$$\begin{aligned}
&\langle\langle \cos^2\theta_{lm}\rangle\rangle_{\mathbf{R},\mathbf{R}'\in\hat{A}} \\
&\quad = \left\langle\!\!\left\langle \sum_{i\geqslant \max(l,m)} C_i^2(\mathbf{R}\,|\,\mathbf{R}') \Big/ \sum_{i\geqslant \min(l,m)} C_i^2(\mathbf{R}\,|\,\mathbf{R}') \right\rangle\!\!\right\rangle_{\mathbf{R},\mathbf{R}'\in\hat{A}} \\
&\quad \approx \sum_{i\geqslant \max(l,m)} C_i^2 \Big/ \sum_{i\geqslant \min(l,m)} C_i^2 \qquad (6.4)
\end{aligned}$$

As $|l-m|\to\infty$, the above quantity goes to zero and the two vectors become perpendicular. Now we evaluate how it decreases with $|l-m|$. For $i\gg I_{LC}$ we know that C_i^2 decreases algebraically as $C_i^2\propto i^{-2\eta}$, but for $i<I_{LC}$ we do not know a precise analytical expression. However, empirical study shows that it is roughly expressed by an exponential function, i.e., $C_i^2\propto \exp(-\gamma i)$, where γ is a constant. Therefore, the types of decay in

$\langle\langle\cos^2\theta_{lm}\rangle\rangle$ are quite different depending on whether $l, m < I_{LC}$ or not. For $l, m < I_{LC}$ we obtain

$$\langle\langle\cos^2\theta_{lm}\rangle\rangle \sim \exp -\gamma\,|l-m| \tag{6.5a}$$

whereas for $l, m > I_{LC}$

$$\langle\langle\cos^2\theta_{lm}\rangle\rangle \approx [\min(l, m)/\max(l, m)]^{2\eta-1} \tag{6.5b}$$

Now we introduce a quantity $n_L(l)$ characterizing the number of projected vectors similar to the lth projected one. This is defined as the total number of vectors such that $\langle\langle\cos^2\theta_{lm}\rangle\rangle \leqslant 1/2$, i.e., $\langle\langle|\theta_{lm}|\rangle\rangle \leqslant \pi/4$. Thus $n_L(l)$ is evaluated as

$$n_L(l) = \text{const.} \qquad \text{for} \quad l < I_{LC} \tag{6.6a}$$

$$n_L(l) = (2^{1/2\eta-1} - 2^{-1/2\eta-1})l \qquad \text{for} \quad l > I_{LC} \tag{6.6b}$$

Equations (6.6) explains the linear growth of correlation length $\Delta_L(l)$ which occurs for $l > I_{LC}$ (see Fig. 6a), because the similarity between the two projected vectors should be reflected in an enhancement of correlation between their square component. There is, however, a big quantitative discrepancy between $n_L(l)$ and $\Delta_L(l)$: The rate of increase, i.e., $dn_L(\Delta)/dl$, typically 0.5 or so ($\eta = 1.8$), is much smaller than that of $\Delta_L(l)$, which is roughly $d\Delta_L(l)/dl \approx 1.8$.

To explain the above discrepancy we have to take into account the localization effect. To describe this effect we introduce the flatness factor for the time series $\psi_l^2(\tau, \mathbf{R}\,|\,\mathbf{R}')$

$$\begin{aligned} F_L(l) &= \langle\langle\overline{\psi_l^4(\tau, \mathbf{R}\,|\,\mathbf{R}')}/\overline{\psi_l^2(\tau, \mathbf{R}\,|\,\mathbf{R}')}^2\rangle\rangle_{\mathbf{R},\mathbf{R}'\in\hat{A}} \\ &\approx \langle\langle\overline{\psi_l^4(\tau, \mathbf{R}\,|\,\mathbf{R}')}\rangle\rangle_{\mathbf{R},\mathbf{R}'\in A}/\langle\langle\overline{\psi_l^2(\tau, \mathbf{R}\,|\,\mathbf{R}')}^2\rangle\rangle_{\mathbf{R},\mathbf{R}'\in\hat{A}} \end{aligned} \tag{6.7}$$

Suppose that the time series $\psi_l^2(t)$ is localized in some time domains (active domains) with a characteristic amplitude ψ_{av}^2, the flatness factor leads to

$$\begin{aligned} F_L(l) &\approx \frac{\psi_{\text{av}}^4 \times \sum(\text{length of active domain}) \times t_R}{[\psi_{\text{av}}^2 \times \sum(\text{length of active domain})]^2} \\ &= t_R \Big/ \sum(\text{length of active domain}) \end{aligned}$$

Thus the flatness factor characterizes the reciprocal of the fraction of active domains filled with the fluctuation. From eq. (6.7) we obtain the relation $F_L(l) = C_{ll}^L + 1$, so that we can read $F_L(l)$ from the peak value of the

correlation function. As seen from Fig. 6(a) the flatness factor increases linearly with l, which implies a development of localization with l. Suppose $m \gg l$. Then the inequality

$$\langle\langle \overline{\psi_l^2 \psi_m^2} \rangle\rangle \approx \langle\langle \overline{(\psi_l - \psi_m)^2 \psi_m^2 + \psi_m^4} \rangle\rangle \gg \langle\langle \psi_m^4 \rangle\rangle$$

leads to

$$C_{lm}^L \gg F_L(m) \langle\langle \cos^2 \theta_{lm} \rangle\rangle - 1 \tag{6.8}$$

The above inequality means that C_{lm}^L decays much slower than $\langle\langle \cos^2 \theta_{lm} \rangle\rangle$ does. Thus $\Lambda_L(l)$ should be much larger than $n_L(l)$. The localization phenomenon is attributed to the nature of the Lyapunov vectors rather than that of the Lyapunov component (see Appendix B). However, we do not go any further into this problem in the present paper. This problem will be discussed elsewhere.

Now we summarize the important result of this section.

Short Summary 3. The exterior subspaces of attractor are defined using the Lyapunov basis. The correlation characteristics of the state vectors projected onto different exterior subspaces change markedly as these exteriors "go out" of the attractor.

7. LYAPUNOV–FOURIER (L–F) CORRESPONDENCE

The Lyapunov exponents agree with the decay rates of linear fluctuation modes as the order exceeds I_{LE}. For such vector numbers it seems quite plausible that the Lyapunov vectors have some resemblance to the linear fluctuation modes that are well-approximated by the Fourier vectors. To examine this idea, we computed the square average of the inner product of a Lyapunov vector with a Fourier vector

$$P_L(i|k) = \langle\langle (\mathbf{e}_i(\mathbf{R}') \cdot \mathbf{f}_K)^2 \rangle\rangle_{\mathbf{R}' \in \hat{A}} \tag{7.1}$$

This quantity measures the contribution from $\mathbf{e}_i$ to $\mathbf{f}_k$ (and vice versa). In Fig. 7(a) we indicate by circles the $i = i_{\max}(k)$ maximizing $P_L(i|k)$ for a given k. The shaded region indicates the range of i satisfying $P_L(i|k) \geqslant 0.7 P_L[i_{\max}(k)|k]$ for a given k. Figure 7(a) means that the vector numbers of Lyapunov vectors chiefly contributing to $\mathbf{f}_k$ are localized in the vicinity of $i_{\max}(k) \approx k$, and thus there is a statistical one-to-one correspondence between the Fourier vectors and the Lyapunov vectors. A surprising fact is that such correspondence exists even for the Lyapunov vectors whose order is smaller than I_{LE}. Strictly speaking, this correspondence rule breaks down for a small k regime where $i_{\max}(k) = 1$. Such Fourier modes correspond to

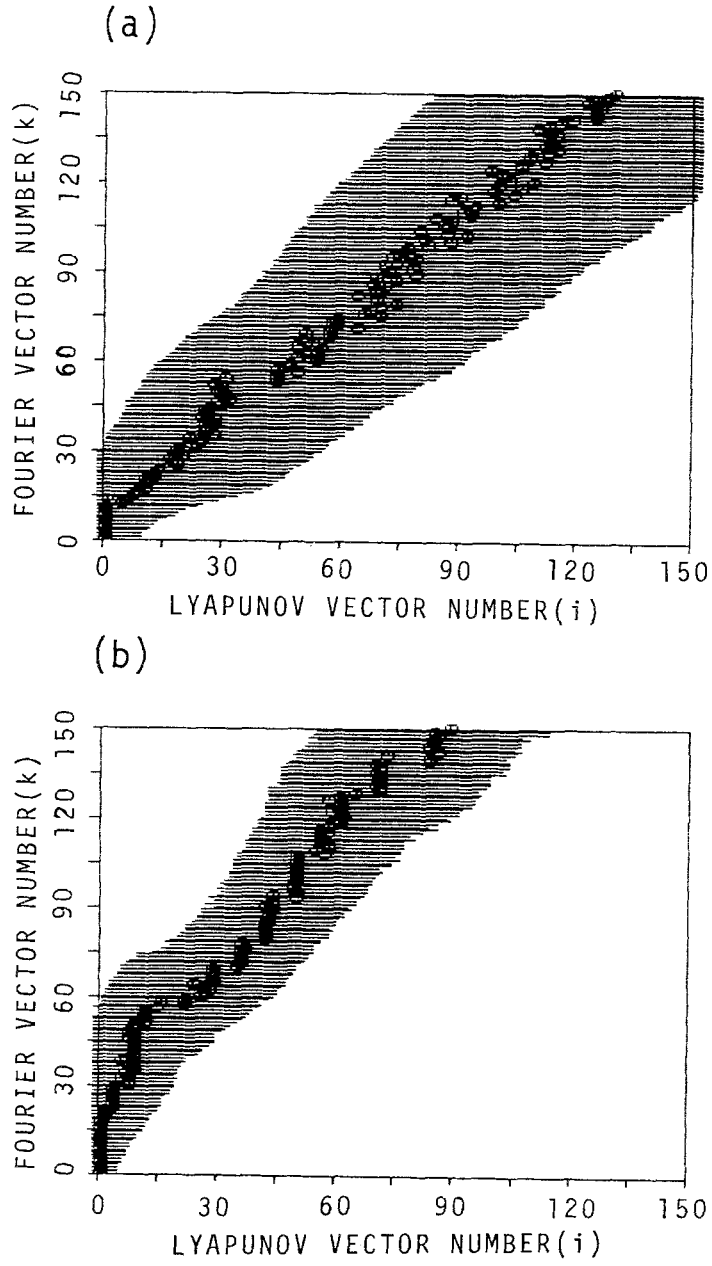

Fig. 7. Lyapunov–Fourier (L–F) correspondence; (a) correspondence between the Lyapunov basis and the Fourier basis, (b) correspondence between projected vectors. See the text.

the core vectors discussed in the previous section, and we call them the "core modes" because they carry the major part of turbulent fluctuation. The total number of core modes is much smaller than D and I_{LE}. The meaning of core modes is discussed in Appendix B in connection with the recent results on Kuramoto–Sivashinski equation.

The correspondence rule between the Lyapunov basis and the Fourier basis ensures that the correlation characteristics of the projected vectors onto the exteriors, which have been discussed in the previous section, must be observed also on the Fourier basis. However, the correspondence rule for the projected vectors is considerably different from that for the basis as shown below. Consider the projection of a state vector onto the external subspace defined by the Lyapunov basis. We rewrite it in terms of the Fourier basis

$$\hat{P}_l^L(\mathbf{R}')\mathbf{R} = \sum_q \tilde{F}_q(\mathbf{R}\,|\,\mathbf{R}')\,\mathbf{f}_q \tag{7.2}$$

with

$$\tilde{F}_q(\mathbf{R}\,|\,\mathbf{R}') \equiv \sum_{j \geqslant l} G(q, j, \mathbf{R}\,|\,\mathbf{R}') \tag{7.3a}$$

and

$$G(q, j, \mathbf{R}\,|\,\mathbf{R}') \equiv (\mathbf{e}_j(\mathbf{R}') \cdot \mathbf{f}_q) \cdot C_j(\mathbf{R}\,|\,\mathbf{R}') \tag{7.3b}$$

Let us define the square average $P_{FL}(i\,|\,k) \equiv \langle\langle G^2(k, j, \mathbf{R}\,|\,\mathbf{R}')\rangle\rangle_{\mathbf{R},\mathbf{R}' \in \hat{A}}$. Then

$$P_{FL}(i\,|\,k) = P_L(i\,|\,k)\, C_i^2 \tag{7.4}$$

Figure 7(b) shows the order $i = i^*(k)$ maximizing $P_{FL}(i\,|\,k)$ and the range of i satisfying $P_{FL}(i\,|\,k) \geqslant P_{FL}(i^*(k)\,|\,k) \times 0.7$. Except for small k corresponding to the core mode, $i^*(k)$ is approximated by a linear function of k

$$i^*(k) = A_0 + A_1 k \tag{7.5}$$

Since the Lyapunov component takes the maximum at $i = 1$, $i^*(k)$ shifts to the lower side of $i_{\max}(k)$, and so $A_1 \leqslant 1$. According to numerical computations the function $i^*(k)$ is not very sensitive to the parameters μ and t_R. Typical values of the two coefficients are $A_0 \sim t_R/\pi$ and $A_1 \sim 0.5$–0.7.

Relation (7.5) provides a modified correspondence rule: For a given k, $P_{FL}(i\,|\,k)$ is well-localized around $i = i^*(k)$. Hence we can approximate $\tilde{F}_q(\mathbf{R}\,|\,\mathbf{R}')$ by $F_q(\mathbf{R})$ for $q \gg i^{*-1}(l)$ and by 0 for $q \ll i^{*-1}(l)$, respectively. Thus we have the following correspondence

$$\hat{P}_l^L(\mathbf{R}')\mathbf{R} \approx \sum_{q > i^{*-1}(l)} F_q(\mathbf{R})\,\mathbf{f}_q \equiv \hat{P}^F_{i^{*-1}(l)}\mathbf{R} \tag{7.6}$$

The operator $\hat{P}_k^F$, which is a counterpart of $\hat{P}_l^L$, is an operator projecting a vector onto the subspace spanned by the Fourier vectors ($\mathbf{f}_k$, $\mathbf{f}_{k+1}$, $\mathbf{f}_{k+2}$,...). The component of the vector $\hat{P}_k^F\mathbf{R}$ at time τ is

$$\psi_k(\mathbf{R}, \tau) = \sum_{q \geq k} F_q(\mathbf{R}) f_q(\tau) \tag{7.7}$$

Since $f_q(\tau)$ is the Fourier mode, $\psi_k(\mathbf{R}, t)$ is nothing but a time series passed through a high-pass filter with the lower cutoff frequency $\omega_k = kt_R/\pi$ (for k even) or ω_{k+1} (for k odd). (See eq. (3.2).)

To summarize the result of present section.

Short Summary 4. Except for the core mode, each of the Lyapunov vectors has a statistical one-to-one correspondence with each of the Fourier vectors.

8. HIGHPASS-FILTERED TIME SERIES

According to the suggestion in the previous section, we study here characteristics of the high-pass filtered time series (HFTS) $\psi_k(\mathbf{R}, t)$. The results presented here are not always based on the HFTS constructed from the Fourier transformation defined by eq. (3.3); we often choose the sample length for the Fourier transformation much longer than t_R. However, the final result thus obtained is insensitive to the choice of sampling length. In this case the lower cutoff frequency of the high-pass filtered time series and the number k in eq. (7.7) are related by $k = [\omega t_R/\pi]$, because two Fourier modes exist in the frequency interval $2\pi/t_R$ (see eq. (3.2)). We show in Fig. 8 a few examples of the HFTS for different cutoff frequencies $\omega = k\pi/t_R$. At low frequencies the HFTS is almost entirely filled with fluctuation. However, as the cutoff frequency increases the HFTS becomes localized in several time domains, forming a "burst" of fluctuations. To visualize this we show how the active time domains are distributed over a two-dimensional plane of τ and ω. An example is depicted in Fig. 9. For a given ω the active time domains, which are defined as a domains of τ satisfying $\psi_k^2(\mathbf{R}, \tau) \geq \psi_k^2(\mathbf{R})$ ($\equiv$average of $\psi_k^2(\mathbf{R}, \tau)$ over τ) are indicated by lines. The distribution pattern of active domains is quite different in the high-frequency regime than in the low-frequency regime; in the former, active domains at different frequencies are strongly connected with each other, whereas in the latter such a connectivity disappears and the distribution of active domain has an irregular pattern.

To describe the above characteristics quantitatively, we introduce the correlation function C_{kq}^F between the two HFTS $\psi_q^2(\mathbf{R}, t)$ and $\psi_k^2(\mathbf{R}, t)$. The definition of C_{kq}^F is the same as C_{lm}^L (see eq. (6.3). We depict the correlation

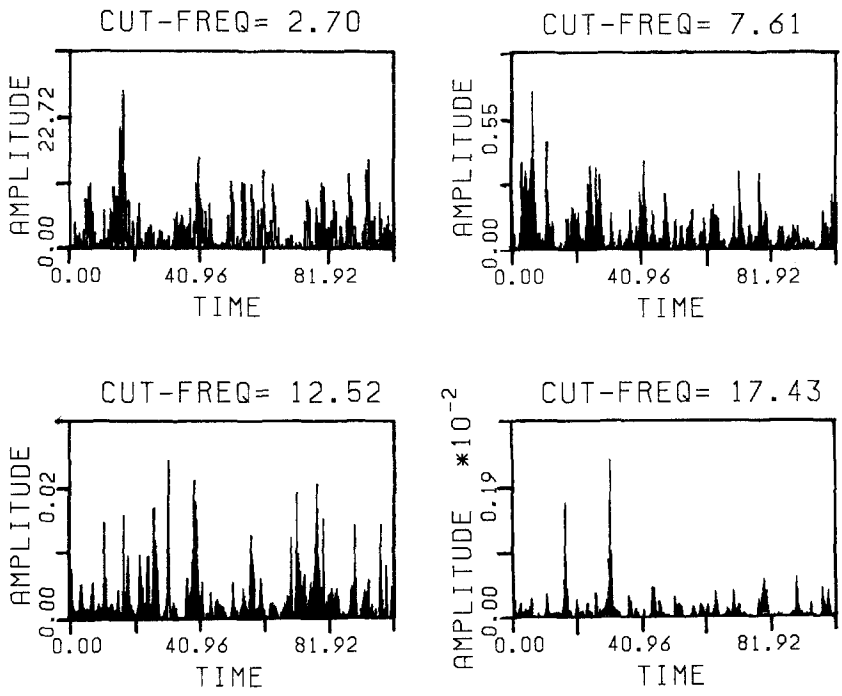

Fig. 8. High-pass filtered time series for various lower cutoff frequencies. Here $\mu = 2.10$ and $t_R = 20$.

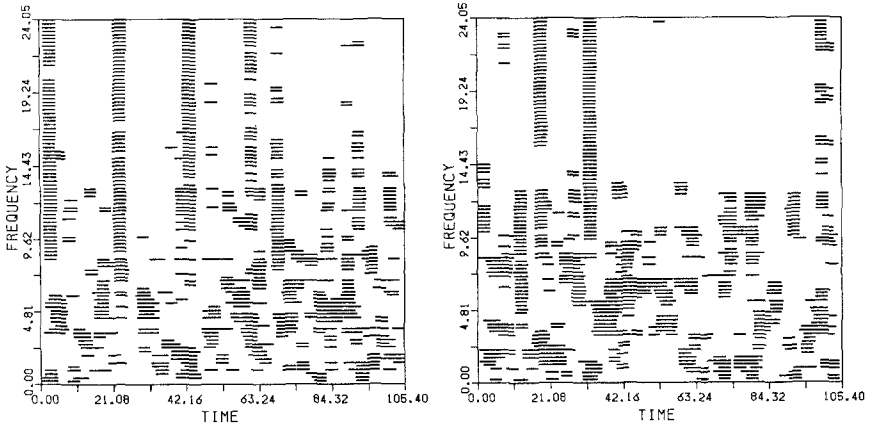

Fig. 9. Distribution of active time domains of high-pass filtered time series on the plane of time and cutoff frequency. Here $\mu = 2.10$ and $t_R = 20$.

functions at various k in Fig. 10(a). For a given k, C_{kq}^F has a maximum at $q=k$. Observe that the right-hand-side of C_{kq}^F has a long tail for k exceeding some critical value. To describe this we define the correlation length $\Delta_F(k)$ at a given k as the half-width of C_{kq}^F. Figure 10(b) shows the behavior of $\Delta_F(k)$. Certainly, the correlation length increases very rapidly as k exceeds a characteristic value K_{FC}. The frequency $\omega_{FC}=K_{FC}\pi/t_R$ is the border of the two regimes in Fig. 9.

The two frequency regimes $\omega<\omega_{FC}$ and $\omega>\omega_{FC}$ should correspond to the interior and the exterior of the attractor, respectively. Thus the critical value K_{FC} must be the counterpart of the characteristic order I_{LC} discussed in Sections 5 and 6. To verify this we check whether the correspondence rule $I_{LC}=i^*(K_{FC})$ (eq. (7.5)) is satisfied or not. In Fig. 11 we compare K_{FC} with $i^{*-1}(I_{LC})$ for various sets of parameters μ and t_R. The agreement is quite satisfactory. Here K_{FC} and I_{LC} are determined from different time series for a given set of parameters t_R and μ. The function $i^*(x)$ is constructed numerically according to the procedures explained in Section 7. Roughly it is approximated by a linear function

$$i^*(x)=0.5x$$

Since I_{LC} is related to the Lyapunov dimension D by eq. (5.5), K_{FC} is roughly proportional to D

$$K_{FC}/D\approx 1.5$$

This implies that the Fourier space is about 1.5 times more "redundant" than the Lyapunov space in confining the attractor.

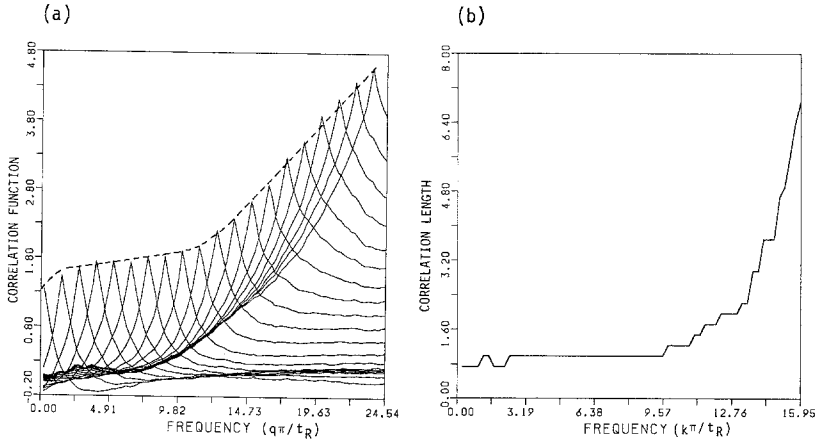

Fig. 10. Correlation functions C_{kq}^F, (a) at various k and (b) correlation length $\Delta_F(k)$. In (a) the broken curve indicates (flatness factor -1) at q. Here $\mu=2.10$ and $t_R=20$. Compare with Fig. 6.

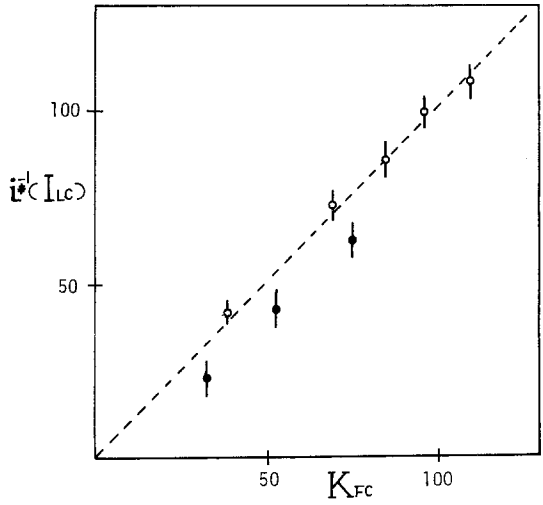

Fig. 11. Test of the L–F correspondence for various sets of parameters μ and t_R. See the text.

As will be discussed in Appendix B, the Fourier spectrum, i.e., $\langle\langle F_q(\mathbf{R})^2\rangle\rangle_{\mathbf{R}\in\hat{A}}$, decays exponentially in the high-frequency range. Such a frequency range is usually called the dissipative range. At first sight the dissipative range seems to correspond to the exterior of the attractor. However, this is not the case—at least in our system—because ω_{FC} is in the midst of the dissipative range, and there is not a clear indication that the shape of spectrum changes in the vicinity of ω_{FC}. Thus the averaged Fourier component itself contains little information about the attractor in contrast with the averaged Lyapunov component.

Kraichnan first suggested that the high-pass filtered time series becomes localized in the dissipative range.[10] Such a localization is often called the dissipative range intermittency. Recently Morf and Frisch proposed an interpretation of the intermittent burst in terms of the complex time singularity.[11] As discussed in Section 6, the degree of intermittency is measured by the flatness factor, which is given by the maximum value of the correlation function C_{kk}^f plus 1 (see Sect. 6). As is seen in Fig. 10(a), the flatness factor certainly increases; however, it does not increase significantly until ω exceeds ω_{FC}, although ω_{FC} is in the midst of the dissipative range. Thus the localization occurs simultaneously with the rapid growth of correlation length. An important fact is that there is a low-frequency range in which the flatness does not increase significantly, which corresponds to the interior of the attractor. Such a behavior has been observed also in an experiment on fluid turbulence (see Fig. 16 of Ref. 12).

This fact holds out hope that information on the strange attractor of fluid turbulence may be obtained directly from the HFTS.

To summarize:

Short Summary 5. The high-pass filtered time series provides direct information about the exterior and interior of the attractor.

9. CONCLUSION

In the present paper we examined several methods to characterize the nature of a high-dimensional chaotic attractor. Using these methods, we investigated the underlying mechanism which connects the physical processes of turbulence occurring in the real space with the characteristics of the attractor in the phase space. In particular, we introduce the ideas of "interior" and "exterior" of the attractor, using the Lyapunov basis. The chaotic motion observed from the "interior" is considerably different from that observed from the "exterior." We have shown that the above difference is dramatically reflected in the correlation characteristics of the high-pass filtered time series, which is clearly represented by the pattern of the distribution of active time domains (Fig. 9).

The main results of Sections 4–8 are summarized in the form of a short summary at the end of each section. Each of these results expresses an important property of our high-dimensional attractor, and summary 5, which states the nature of high-pass filtered time series, has been derived as a natural result of summaries 1–4. It seems probable that all the assertions in the summaries hold well only for the delay-differential equations. However, we believe that it is worthwhile to examine the validities of these assertions in other high-dimensional attractors. In this sense we propose these assertions as *working hypotheses* to be examined in other attractors.

Although the universality of assertions 1–4 may be doubtful, the assertion in 5 seems to be quite plausible and might be valid for a considerably wide class of high-dimensional attractors. The reason is quite simple: In the interior of an attractor new information, in other words, a new temporal pattern, is generated continuously. This information is transported to the exterior of the attractor and dies away there. Generally speaking, the high-frequency (or wave number) mode corresponds to the exterior of the attractor. If the lower cutoff frequency (or wave number) k of the high-pass filtered temporal (or spatial) signal is large enough, the high-pass filtered signal contains only the information in the exterior of the attractor, and so the pattern of the high-pass filtered signal is insensitive to the variation of k. However, as k becomes smaller, the high-pass filtered signal involves new information generated in the interior of the attractor, and the pattern

of the high-pass filtered signal becomes rich in new patterns and thus is sensitive to k.

To verify the above conjecture we have to investigate the processes of generation and transport of information in high-dimensional attractors. This will be described in a forthcoming publication.

APPENDIX A: NUMERICAL METHODS

A.1. Integration of Delay-Differential Equation

Equation (2.6) is equivalent to

$$\begin{aligned} x_{n+1}(\tau) &= F[x_n(\tau), x_{n+1}(\tau)] \\ &\equiv -x_{n+1}(\tau) + \pi\mu f[x_n(\tau)] \end{aligned} \tag{A1}$$

Let us denote the mth derivative of $x_n(\tau)$ and of $x_{n+1}(\tau)$ by $p^{(m)}(\tau)$ and $q^{(m)}(\tau)$, respectively. The mth derivative $q^{(m)}(\tau)$ can be expressed in terms of $q^{(0)}(\tau)$ and $p^{(m')}(\tau)$ $(0 \leqslant m' \leqslant m-1)$. This can easily be shown by differentiating (A1) $(m-1)$ times with respect to τ. For example

$$q^{(1)}(\tau) = F[q^{(0)}(\tau), p^{(0)}(\tau)]$$

$$q^{(2)}(\tau) = F[p^{(0)}(\tau), q^{(0)}(\tau)] \frac{\partial}{\partial q^{(0)}} F[q^{(0)}(\tau), p^{(0)}(\tau)]$$

$$+ P^{(1)}(\tau) \frac{\partial}{\partial p^{(0)}} F[q^{(0)}(\tau), p^{(0)}(\tau)] \qquad \text{etc.}$$

These relations are schematically expressed as

$$q^{(m)}(\tau) = Q^{(m)}[q^{(0)}(\tau), p^{(0)}(\tau), \ldots, p^{(m-1)}(\tau)] \tag{A2}$$

Now we introduce an approximation for numerical integration: We divide section $[0, t_R)$ into N segments of width $h = t_R/N$. Let the kth discrete time be $\tau_k \equiv hk$. The Taylor expansion up to the Mth order leads to

$$q^{(0)}(\tau_{k+1}) \cong \sum_{m=0}^{M} [q^{(m)}(\tau_k)/m!]\, h^m \tag{A3}$$

Equations (A2) and (A3) together with the continuity condition

$$q^{(0)}(\tau_0) = p^{(0)}(\tau_N) \tag{A4}$$

provide a scheme to compute $q^{(m)}(\tau_k)$ $(0 \leqslant m \leqslant M,\ 1 \leqslant k \leqslant N)$ from $p^{(m)}(\tau_k)$ $(0 \leqslant m \leqslant M,\ 1 \leqslant k \leqslant N)$ up to the correction of $O(h^{M+1})$. Replacing all

$p^{(m)}(\tau_k)$ by $q^{(m)}(\tau_k)$ and repeating the above procedure, we can compute $x_n(\tau) = q^{(0)}(\tau)$ successively. In our numerical simulation we typically choose $M = 6$ and $h = 0.05$.

Integration of the variational eq. (2.7) has been done by applying the Runge–Kutta method to the differential equation equivalent to it

$$\delta \dot{x}_{n+1}(\tau) = \frac{\partial F[q^{(0)}(\tau), p^{(0)}(\tau)]}{\partial p^{(0)}(\tau)} \delta x_n(\tau) + \frac{\partial F[q^{(0)}(\tau), p^{(0)}(\tau)]}{\partial q^{(0)}(\tau)} \delta x_{n+1}(\tau) \tag{A5}$$

A.2. Gram–Schmidt Procedure

Consider a set of orthogonal vectors $(\mathbf{e}_1, \mathbf{e}_2, ..., \mathbf{e}_i, ...)$. First we compute the transformed vectors by the variational equation defined by eq. (2.7) or eq. (2.7)′, i.e.

$$\mathbf{a}_i = DF(\mathbf{R}_n)\, \mathbf{e}_i \tag{A6}$$

Next we orthogonalize the vectors $(\mathbf{a}_1, \mathbf{a}_2, ...)$ by Schmidt's method

$$\lambda_1^{(n)} \equiv \|\mathbf{a}_1\| \qquad \text{and} \qquad \mathbf{e}_i' = \mathbf{a}_1/\lambda_1^{(n)}$$
$$\lambda_i^{(n)} \equiv \left\| \mathbf{a}_i - \sum_{j=1}^{i-1} (\mathbf{a}_i \cdot \mathbf{e}_j')\, \mathbf{e}_j' \right\| \tag{A7}$$

and

$$\mathbf{e}_j' = \left[\mathbf{a}_i - \sum_{j=1}^{i-1} (\mathbf{a}_i \cdot \mathbf{e}_j')\, \mathbf{e}_j' \right] \Big/ \lambda_i^{(n)} \qquad (i = 2, 3, ...)$$

Replacing $\mathbf{e}_i$ by $\mathbf{e}_i'$ and $\mathbf{R}_n$ by $\mathbf{R}_{n+1}$, we repeat the above procedure. Then

$$\frac{1}{N} \sum_{n=1}^{N} \log \lambda_i^{(n)} \xrightarrow[N \to \infty]{} \lambda_i \qquad \text{(Lyapunov exponent)}$$

and the orthogonal set of vectors $(\mathbf{e}_1, \mathbf{e}_2, ..., \mathbf{e}_i, ...)$ approaches to the set of Lyapunov vectors defined at R_N.

We carried out the above procedure by means of discrete time representation explained in eq. (A1) ($h = 0.05$ typically). We iterated more than 500 times to attain a sufficient convergence of all the Lyapunov exponents.

APPENDIX B: FOURIER SPECTRUM AND L–F CORRESPONDENCE

The Fourier spectrum of any dynamical system decays, in general, exponentially in the high frequency (or wave number) regime. Such a frequency regime is usually called the *dissipative range*. On the other hand, the low-frequency regime below the dissipative range we call the *core range*. The greater part of turbulent fluctuation is carried by the Fourier modes in the core range. In the case of our system the Fourier spectrum is empirically given by the following expressions in the limit of $t_R \gg 1$ and $\mu \gg 1$

$$\begin{array}{lll} \text{core range} & \omega \lesssim 1 & P(\omega) \sim 1/1 + \omega^2 \\ \text{dissipative range} & \omega \gg 1 & p(\omega) \sim \exp -\omega/\tilde{\omega} \end{array} \tag{B1}$$

where $\tilde{\omega} = (0.69 \pm 0.07)\mu$. The total number of Fourier modes in the core estimated as $n_c = 1 \div (\pi/t_R) = t_R/\pi$ is much smaller than the Lyapunov dimension $D \approx t_R \mu$ (eq. (4.2)). Thus the core range is completely in the interior of the attractor. As shown in Section 7, a Lyapunov vector with vector number larger than n_c has a corresponding vector in the Fourier basis, i.e., the L–F correspondence, but any Lyapunov vectors with a vector number less than n_c does not. The latter vectors are called the *core Lyapunov vectors* (see Sect. 6). The component of core Lyapunov vector $e_i(\tau, \mathbf{R})$ (see e.q (3.1)) is notably localized in time just as the bound state of a Schrödinger equation with an attractive potential. Therefore, such a vector has the maximum Fourier component at $k = 0$.

On the contrary, the Lyapunov vectors out of the core are extended and oscillate in time just like the ionization states of a Schrödinger equation. Such a state heavily contains a specific Fourier mode and thus has the L–F correspondence.

The core range is very important in the case of the Kuramoto–Sivashinsky (K–S) equation, which has recently been investigated by Pomeau, Pumir, and Pelce[5] and by Manneville, Pumir, and Tuckerman.[5] Contrary to our model, the core range is relatively wider and the wave number corresponding to D is in the midst of the core range. According to the results of Pomeau, Pumir, and Pelce[5] there is no indication of the L–F correspondence when the Lyapunov vector number is smaller than D. It seems that such Lyapunov vectors are localized in space.[5] Considering these, the frequency (or wave number) range where the L–F correspondence exists may be closely connected with the dissipative range. In Fig. 12 we summarize what is known and also what may be conjectured for the K–S equation in comparison with our model equation.

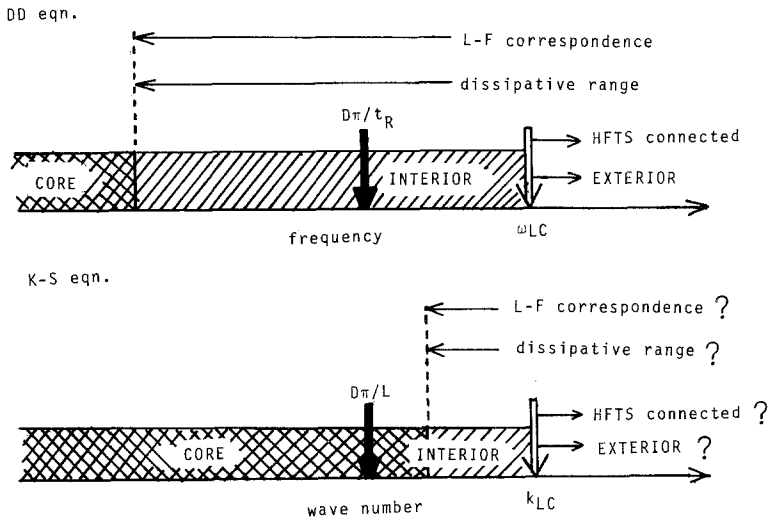

Fig. 12. Relation between structure of attractor and phenomena occurring in frequency (wave number) space, which is established for the delay-differential (DD) equation and expected for the Kuramoto–Sivashinsky (K–S) equation.

REFERENCES

1. A. S. Monin, *Sov. Phys. Usp.* **21**:429 (1978); J. P. Eckmann, *Rev. Mod. Phys.* **53**:643 (1981); R. H. G. Helleman, in W. Horton, L. Reichl, and V. Szebehely, eds., *Long-time Prediction in Dynamics*, p. 95 (John Wiley & Sons, New York, 1982).
2. E. N. Lorenz, *J. Atmos. Sci.* **20**:130 (1963); J. B. McLaughlin and P. C. Martin, *Phys. Rev. A* **12**:186 (1975); H. Yahata, in Y. Kuramoto, ed., *Chaos and Statistical Methods*, p. 232 (Springer, Berlin, 1984).
3. A. S. Monin and A. M. Yaglom, *Statistical Fluid Mechanics* (MIT Press, Cambridge, 1975); T. Tatsumi, *Adv. Appl. Phys.* **20**:39 (1980).
4. J. D. Farmer, *Physica* **4D**:336 (1982).
5. Y. Pomeau, A. Pumir, and P. Pelce, *J. Stat. Phys.* **37**:39 (1984); P. Manneville, A. Pumir, and L. Tuckerman, preprint.
6. K. Ikeda, *Opt. Commun.* **30**:257 (1979); K. Ikeda, H. Daido, and O. Akimoto, *Phys. Rev. Lett.* **45**:709 (1980); K. Ikeda and O. Akimoto, in Y. Kuramoto, ed., *Chaos and Statistical Methods*, p. 249 (Springer, Berlin, 1984).
7. K. Ikeda and O. Akimoto, in L. Mandel and E. Wolf, eds., *Coherence and Quantum Optics V*, p. 701 (Plenum, New York, 1984).
8. V. I. Oseledec, *Trans. Moscow Math. Soc.* **19**:197 (1968); I. Shimada and T. Nagashima, *Prog. Theor. Phys.* **61**:1605 (1979).
9. J. Kaplan and J. Yorke, in H. O. Pietgen and H. O. Walther, eds., *Functional Differential Equations and Approximations of Fixed Points* (Springer, Berlin/New York, 1979).
10. R. H. Kraichnan, *Phys. Fluids* **10**:2080 (1967).
11. U. Frisch and R. Morf, *Phys. Rev. A* **23**:2673 (1981).
12. A. Y. Kuo and S. Corrsin, *J. Fluid Mech.* **50**:285 (1971).